Title

Spectral fitting strategy to overcome the overlap between 2-hydroxyglutarate and lipid resonances at 2.25 ppm.

Journal

Magnetic Resonance in Medicine, 86(4)

Authors

Askari, Pegah
Dimitrov, Ivan
Ganji, Sandeep
et al.

Publication Date

2021-10-01

DOI

10.1002/mrm.28829

Peer reviewed

HHS Public Access

Author manuscript

Magn Reson Med. Author manuscript; available in PMC 2022 October 01.

Published in final edited form as:

Magn Reson Med. 2021 October ; 86(4): 1818–1828. doi:10.1002/mrm.28829.

Spectral fitting strategy to overcome the overlap between 2-hydroxyglutarate and lipid resonances at 2.25 ppm

Pegah Askari[1,2], **Ivan E. Dimitrov**[1,3], **Sandeep K. Ganji**[4,5], **Vivek Tiwari**[1], **Michael Levy**[6], **Toral R. Patel**[6,7,8], **Edward Pan**[7,9], **Bruce E. Mickey**[6,9,10], **Craig R. Malloy**[1,5,11], **Elizabeth A. Maher**[7,9,10,12], **Changho Choi**[1,5,9]

[1]Advanced Imaging Research Center, University of Texas Southwestern Medical Center, Dallas, Texas

[2]Joint Graduate Program in Biomedical Engineering at University of Texas Arlington and University of Texas Southwestern Medical Center, Texas

[3]Philips Healthcare, Gainesville, Florida

[4]Philips Healthcare, Andover, Massachusetts

[5]Department of Radiology, University of Texas Southwestern Medical Center, Dallas, Texas

[6]Department of Neurological Surgery, University of Texas Southwestern Medical Center, Dallas, Texas

[7]Department of Neurology and Neurotherapeutics, University of Texas Southwestern Medical Center, Dallas, Texas

[8]Department of Radiation Oncology, University of Texas Southwestern Medical Center, Dallas, Texas

[9]Harold C. Simmons Cancer Center, University of Texas Southwestern Medical Center, Dallas, Texas

[10]Annette G. Strauss Center for Neuro-Oncology, University of Texas Southwestern Medical Center, Dallas, Texas

[11]Veterans Affairs North Texas Health Care System, Dallas, Texas

[12]Department of Internal Medicine, University of Texas Southwestern Medical Center, Dallas, Texas

Abstract

Purpose: ^{1}H MRS provides a noninvasive tool for identifying mutations in isocitrate dehydrogenase (IDH). Quantification of the prominent 2-hydroxyglutarate (2HG) resonance at 2.25 ppm is often confounded by the lipid resonance at the same frequency in tumors with

Correspondence: Changho Choi, Advanced Imaging Research Center, University of Texas Southwestern Medical Center, 5323 Harry Hines Blvd., Dallas, Texas 75390-8542. Changho.Choi@UTSouthwestern.edu.
Current address: Centre for Brain Research, Indian Institute of Science, Bangalore, India

elevated lipids. We propose a new spectral fitting approach to separate these overlapped signals, thus improving 2HG evaluation.

Methods: TE 97ms PRESS was acquired at 3T from 42 glioma patients. New lipid basis sets were created, in which the small lipid 2.25-ppm signal strength was preset with reference to the lipid signal at 0.9 ppm, incorporating published fat relaxation data. LCModel fitting using the new lipid bases (Fitting method 2) was conducted along with fitting using the LCModel built-in lipid basis set (Fitting method 1), in which the lipid 2.25-ppm signal is assessed with reference to the lipid 1.3-ppm signal. In-house basis spectra of low-molecular-weight metabolites were used in both fitting methods.

Results: Fitting method 2 showed marked improvement in identifying IDH mutational status compared with Fitting method 1. 2HG estimates from Fitting method 2 were overall smaller than those from Fitting method 1, which was due to differential assignment of the signal at 2.25 ppm to lipids. In receiver operating characteristic analysis, Fitting method 2 provided a complete distinction between IDH mutation and wildtype while Fitting method 1 did not.

Conclusion: The data suggest that ^{1}H MR spectral fitting using the new lipid basis set provides a robust fitting strategy that improves 2HG evaluation in brain tumors with elevated lipids.

Keywords

2-Hydroxyglutarate (2HG); Lipids (Lip); ^{1}H MRS; IDH mutation; 3T; TE 97 ms PRESS

INTRODUCTION

2-Hydroxyglutarate (2HG), which is normally present in vanishingly small quantities in the human brain, is elevated to millimolar levels in gliomas with mutations in isocitrate dehydrogenase (IDH) 1 and 2 genes.[1] Clinical significance of IDH mutation is manifested in its association with long survival.[2, 3] The IDH mutational status is established as a primary factor in glioma classification.[4] Noninvasive identification of 2HG in glioma patients using MR spectroscopy[5–7] therefore provides a biomarker of IDH mutation, improved prognosis, and glioma classification. Clinical trials are in progress to test IDH inhibitors for potential therapy in IDH mutant glioma patients,[8, 9] and thus 2HG MRS can play an important role in developing therapeutics for IDH mutant gliomas. Taken together, accurate MRS evaluation of 2HG levels in brain tumor patients is pivotal in glioma patient management.

Lipid levels can be elevated due to tumor progression and necrosis[10, 11] and consequently MR spectra from high-grade brain tumors often show elevated signals from mobile lipids. In ^{1}H MRS, six lipid resonances are present between 0 and 4 ppm,[10–13] which is a spectral region of interest in many MRS studies. The most prominent lipid signals, arising from the CH_2-chain and CH_3 protons, appear at 1.3 and 0.9 ppm, respectively. Other four resonances, all arising from single-methylene units, are present between 1.6 and 2.8 ppm. The resonances at 2.0 and 2.8 ppm are attributed to methylene protons α to double-bond carbon (−C$\mathbf{H_2}$−CH=CH−) and diallylic methylene protons (=CH−C$\mathbf{H_2}$−CH=), respectively (Figure 1A), and thus their signal strengths depend upon the specific contents of mono-unsaturated and poly-unsaturated fats in the brain tumor.[12] The lipid resonances at 2.25 and 1.6 ppm arise from the methylene protons α to carboxyl group (−COO−C$\mathbf{H_2}$−) and the methylene

protons β to carboxyl group (−COO−CH_2−C**H_2**−), respectively, and will be present in every fat molecule irrespective of its unsaturation composition, as is the 0.9 ppm resonance.

A 2HG molecule may present proton signals at approximately three locations (4.02, 2.25, and ~1.9 ppm). The 2.25 ppm signal, which is attributed to two adjacent resonances (^{4}C protons), appears to be the largest in commonly available data acquisition methods and thus was a major target signal in many prior 2HG MRS studies. Since the 2HG 2.25 ppm resonance is overlapped with the lipid resonance at 2.25 ppm, evaluation of 2HG using conventional MRS sequences can be complicated when lipid elevation is considerable. Overestimation of 2HG can result when the lipid 2.25 ppm signal is underestimated. As such, false-positive 2HG estimation can occur frequently in high-grade tumors compared with low-grade tumors in which lipid signals are usually negligible.[14, 15] Given the significance of noninvasive identification of the IDH mutational status in high-grade tumors, development of an MRS methodology to overcome the spectral overlap between 2HG and lipids is well warranted.

The lipid signals at 1.3 and 0.9 ppm, which are directly observable in *in vivo* MRS, are much broader than the low-molecular-weight metabolite signals, which is most likely due to T_2 relaxation difference. At 3T, the T_2 of the human tibial bone marrow lipids was measured to be 88 ms using a PRESS sequence[16] while the T_2s of creatine and choline in brain tumors may be as long as 170 – 250 ms.[17, 18] The T_2s of fat signals in the human breast and skeletal adipose tissue were measured to be 30 – 60 ms at 7T,[12, 13] shorter by 2 – 3 fold compared to brain N-acetylaspartate and creatine T_2s at 7T.[19] The lipid 2.25 ppm resonance arising from the methylene group protons showed slightly shorter T_2 than the methyl group proton resonance at 0.9 ppm,[12, 13] (36 *vs.* 41 ms and 55 *vs.* 67 ms for human breast and skeletal fats, respectively). The ratio between the published relaxation times at 7T may be applicable for predicting the lipid signal ratios at long TE at 3T, a field strength widely used for 2HG MRS.

The lipid 2.25 ppm resonance may not be directly identifiable in brain tumors because the signal appears small in a spectrally crowded region. When an indirect assessment of the lipid signal strength is available, accuracy in 2HG evaluation can be improved. In the default spectral fitting by LCModel, which is widely used for ^{1}H MR spectral fitting, the lipid 2.25 ppm signal strength is assessed, using a soft constraint, relative to the major lipid signal at 1.3 ppm, whose signal strength may depend upon fat composition types, thus varying the number of CH_2 chains in tumors. In this paper we present a new fitting approach that can improve the MRS evaluation of 2HG in brain tumors. We utilize that the −COO−CH_2− and −CH_3 units are present in every fatty acid molecule irrespective of its precise lipid nomenclature, and thus the lipid signals at 2.25 and 0.9 ppm arise from number of protons having a constant ratio (*i.e.*, 2:3) in tumors. A new lipid basis signal is constructed for PRESS TE 97 ms, in which the lipid 2.25 and 0.9 ppm resonances are combined into a single basis unit and the 2.25 ppm signal strength is preset with reference to the 0.9 ppm signal incorporating the published T_2 relaxation ratio of the resonances. The new lipid basis set is tested with MRS data from 42 glioma patients. Performance of the new lipid basis set for identifying IDH status is presented in comparison with fitting using the conventional LCModel built-in lipid basis set.

METHODS

Forty-two glioma patients were enrolled in the present study. The enrollment included 20 male and 22 female subjects, with an age range of 20 – 79 years at the time of MRS scans (mean 47±16 years). The tumors included 23 IDH mutated and 19 IDH wildtype gliomas, which were all biopsy proven. The glioma types included 16 glioblastomas, 10 anaplastic astrocytomas, 6 astrocytomas, 2 anaplastic oligodendrogliomas, and 8 oligodendrogliomas. The brain tumor MR protocol was approved by the local Institutional Review Board. Written informed consent was obtained from each patient prior to the MR scan.

^{1}H MR experiments were carried out on a whole-body 3T scanner (Philips Medical Systems), using a body coil for RF transmission and a thirty-two channel phased-array head coil for reception. Following survey imaging, T_2-FLAIR was performed for tumor identification (TR/TE/TI = 9000/125/2600ms; FOV = 230×200 mm^2; slice thickness = 4 mm). Single-voxel localized MRS was acquired with TE 97 ms PRESS (90°−180° pulse interval 16 ms),[5, 20] which had a 9.8-ms 90° pulse (bandwidth 4.2 kHz) and a 13.2-ms 180° RF pulse (bandwidth 1.3 kHz) at an RF field intensity (B_1) of 13.5 μT. The voxel for MRS acquisition was positioned completely within the T_2-FLAIR hyperintensity region, with care taken to avoid cyst, cerebrospinal fluids, and/or resection cavity. The MRS acquisition parameters included a sweep width of 2500 Hz, 2048 sampling points, and a repetition time of 2 s. The number of water-suppressed PRESS signal averages was 128 – 1280, depending upon the voxel size (1.5 – 11.4 mL) (scan time 4 – 43 min). Data were recorded in multiple blocks, each with 16 signal averages. For each block, multi-channel combination and eddy-current compensation were performed with a vendor-supplied tool (Spectral correction). Water suppression was obtained with a four-pulse variable flip angle scheme.[21] First- and second-order shimming for the selected volume was carried out using a vendor-supplied tool (Pencil beam). The B_1 field strength was calibrated on the shimming volume, which was set to be slightly larger than the MRS voxel. The carrier frequency of the PRESS RF pulses was set at 2.7 ppm. The RF frequency of the scanner was adjusted in real time for each excitation using a vendor-supplied tool (Frequency stabilization). In addition, an unsuppressed water signal was acquired with TR 20 s and TE 14 ms for use as reference in metabolite quantification.

The multi-block PRESS spectra were aligned with reference to a total choline (tCho) singlet at 3.21 ppm, prior to averaging the spectra. Following apodization with a 1-Hz exponential function, spectral fitting was performed with LCModel software (Version 6.3-1L).[22] The basis set consisted of low-molecular-weight metabolite basis signals and lipids resonances, excluding macromolecule (MM) resonances. The metabolite basis set included 2HG, glutamate (Glu), glutamine, γ-aminobutyric acid (GABA), myo-inositol, glycine, lactate, citrate, glutathione, alanine, aspartate, ethanolamine, phosphoethanolamine, scyllo-inositol, taurine, glucose, tCho (glycerophosphocholine + phosphocholine), tNAA (N-acetylaspartate + N-acetylaspartylglutamate), and tCr (creatine + phosphocreatine). The metabolite basis spectra were numerically calculated with an in-house density-matrix simulation tool that incorporated the exact shapes of the slice-selective RF and gradient pulses of the PRESS sequence as well as the PRESS subecho times, according to a published product-operator based transformation matrix algorithm (see the Supplementary Methods of reference 5 for

details).[5, 23] A transformation matrix was created for each of the slice-selective 90° and 180° RF pulses and used for metabolite basis signal simulations. The effect of the slice-selective gradient pulse during the RF pulse was incorporated in such a manner that an object length twice larger than slice thickness was divided into 200 even-spaced pixels, in each of which the magnetic field strength was assumed to be uniform. With the RF carrier set at 2.7 ppm, all uncoupled and J-coupled spins in shifted slices that resonate between −1.6 and 7 ppm experienced the PRESS 180° pulses fully and the chemical-shift displacement effects on the coherence evolution of the resonances were taken into account in the transformation matrices and consequently metabolite basis signal calculation, as indicated by phantom data comparison in our prior 2HG MRS study[20]. Published chemical shift and J-coupling constants were used in the simulations.[24] The basis signals of lipids were created using the LCModel built-in tool (Supporting Information, Methods). The LCModel option for data type was set to tumor (*i.e.*, sptype = 'tumor'). Spectral fitting was performed with two methods.

Fitting method 1:

The basis set was composed of in-house calculated metabolite basis and the LCModel default basis of lipid resonances. The lipid basis included Lip20, Lip09, Lip13a, Lip13b. Here Lip09 had a resonance at 0.89 ppm with signal intensity of 3 and the Lip20 contained three resonances at 2.04, 2.25 and 2.8 ppm with signal strengths set at 1.33, 0.67, and 0.87, respectively. The lipid resonances and amplitudes were the LCModel default values.

Fitting method 2:

The basis set included two newly created lipid bases, LipNew1 and LipNew2, in addition to the in-house metabolite basis spectra and the LCModel default basis of the lipid 1.3 ppm resonance (Lip13a and Lip13b). LipNew1 had two resonances at 0.89 and 2.25 ppm, with signal strengths of 3 and 1.8, respectively (Figure 1B). LipNew2 included three resonances at 1.59, 2.04, and 2.8 ppm, with signal strengths of 1.4, 1.7, and 0.6, respectively. The signal strengths of the new Lip basis sets were set according to their signal ratios at TE 97 ms that were calculated incorporating the data in prior 7T fat MRS studies (details shown in Discussion).[12, 13]

The spectral fitting was conducted between 0.2 and 4.0 ppm for both fitting methods with the LCModel default baseline option. Cramer-Rao lower bounds (CRLB) were returned as percentage standard deviation by LCModel. T_2 relaxation effects on metabolite signals at TE 97 ms were corrected using published metabolite T_2 values: T_2 = 180 and 260 for 2HG and tCho, respectively.[18, 25] The concentrations of low-molecular-weight metabolites were quantified in institutional millimolar unit, with reference to water at 48 M[26], ignoring potential differences of the T_1 saturation effect between metabolites and water and potential presence of fluid volumes within the MRS voxels. The 48 M value equaled a white-matter water concentration (40 M) multiplied by an experimental tumor-to-white matter water signal ratio (1.2±0.1, n=14). Lipid levels were assessed in arbitrary unit. Data are presented as mean ± standard deviation (SD).

RESULTS

PRESS TE 97 ms spectra from three representative tumors are presented together with the spectral fitting outputs in Figure 2. A patient with an IDH1 mutated glioblastoma showed a large signal at 2.25 ppm and small lipid signals at 1.3 and 0.9 ppm (Lip13 and Lip09, respectively) (Figure 2A). 2HG was estimated to be 7.4 mM when the LCModel built-in lipid basis set was used in the spectral fitting (Fitting method 1). The LCModel-returned Lip20 signal was essentially null. The Lip09 signal was small and the peak amplitude was 18% relative to the 2HG peak amplitude. When the Lip20 and Lip09 bases were replaced with new lipid bases, LipNew1 and LipNew2 (Fitting method 2), the 2HG estimation was decreased to 6.8 mM, with a slightly increased CRLB (3%) (Figure 2B). The 2.25 ppm signal amplitude of the LCModel-returned LipNew1 was approximately 11% with respect to the amplitude of the fit (green line) at 2.25 ppm. The LCModel-returned lipid 0.9 ppm to 1.3 ppm peak amplitude ratio was 25% and 27% in the Fitting methods 1 and 2, respectively.

A patient with an IDH1 mutated anaplastic oligodendroglioma also showed a large signal at 2.25 ppm. 2HG was estimated to be 7.5 mM using the Fitting method 1 (Figure 2C). The lipid signals in this tumor were much larger compared to the aforementioned IDH mutant glioblastoma. The 1.3 and 0.9 ppm signal amplitudes were both greater by approximately fourfold in this oligodendroglioma than in the glioblastoma. The lipid 0.9 ppm to 1.3 ppm peak amplitude ratio was 33% and 35% in the Fitting methods 1 and 2, respectively. The ratio of the Lip20 signal at 2.25 ppm with respect to the LCModel-returned 2HG peak was 15%. 2HG estimation using Fitting method 2 was drastically reduced (4.3 mM) most likely due to the presence of a large lipid signal at 2.25 ppm (Figure 2D). A large LipNew1 signal was returned in the LCModel fitting. The LipNew1 peak at 2.25 ppm was as high as the LCModel-returned 2HG peak (95%), suggesting that the 7.5 mM 2HG from the Fitting method 1 could be an overestimation arising from suboptimal differentiation between the overlapping 2HG and lipid signals at 2.25 ppm. The estimates of Glu and GABA in the tumors were not very different between the fitting methods (Supporting Information Figure S1).

Next, an IDH wildtype glioblastoma showed a very high lipid signal at 1.3 ppm but a relatively small peak at 0.9 ppm (Figure 2E). The 0.9 ppm to 1.3 ppm lipid peak amplitude ratio was as small as 7 – 8% in this glioblastoma, approximately fourfold smaller compared with the two aforementioned tumors. Fitting method 1 resulted in 1.0 mM 2HG. Reduction of 2HG estimation by Fitting method 2 also occurred in this tumor, leading to a negligible estimation of 2HG (0.1 mM) (Figure 2F). The LCModel-returned LipNew1 had a considerable signal at 2.25 ppm, which was likely assigned to 2HG in Fitting method 1.

For the three cases in Figure 2, the tCho singlet linewidths at half amplitude were 6 – 8 Hz (following the apodization with a 1-Hz exponential function) and the tCho singlet to background noise ratios (SNR) were 120 – 150, where the background noise was the standard deviation of the fitting residuals between 0.2 and 4.0 ppm. The spectra from the 42 patients of the present study are shown in Supporting Information Figure S2. Due to substantial attenuation of MM signals and the J-coupled spin coherence evolution during the 97 ms TE, metabolite signals were well discernible on nearly flat baselines. The classic

pattern of elevated tCho with decreased and tNAA was present in all spectra. The tCho-to-tNAA concentration ratio ranged from 0.4 to 3.0 (mean 1.1±0.7), much higher than healthy-brain values (~0.1). For the 42 MRS voxels, whose size ranged from 1.5 to 11.4 mL (mean 6.0±2.2 cm^3), the tCho singlet linewidth and SNR ranged from 4.0 to 9.8 Hz (mean 6.6±1.3 Hz) and from 41 to 203 (mean 107±44), respectively. The mean tCho concentration in the 42 tumors was 2.4±1.4 mM, ranging from 1.0 to 7.3 mM. The linewidth of the unsuppressed water signals from the voxels was smaller than the tCho linewidth, ranging from 2.0 to 7.6 Hz (mean 4.6±1.4 Hz). In addition, the tCho linewidth was slightly larger in low-2HG tumors (< 0.4 mM; P1 – P19) than in high-2HG tumors (> 0.8 mM; P20 – P42) (*i.e.*, 7.5±1.5 vs. 6.1±1.0 Hz).

As shown in the three representative cases shown earlier, use of the new lipid basis sets for spectral fitting (Fitting method 2) resulted in a decrease in 2HG estimation in most cases, compared with the 2HG estimation by Fitting method 1 (Figure 3A). For the 42 tumors, the difference between the 2HG estimates from the two fitting methods, *i.e.*, $[2HG]_{\text{Fitting method 2}} - [2HG]_{\text{Fitting method 1}}$, ranged from −3.2 mM to +0.2 mM, depending upon the lipid 0.9 ppm signal strength. A regression analysis showed that reduction in 2HG estimation was significantly associated with the lipid 0.9 ppm signal strength ($p = 7\times10^{-9}$) (Figure 3B). For 14 tumors that showed clearly discernible lipid signals at 0.9 ppm (SNR > 4), the lipid 0.9 ppm to 1.3 ppm peak amplitude ratio differed across the tumors substantially (8% – 35%) (Figure 3C). The lipid 0.9 ppm to 1.3 ppm peak area ratio also differed across the tumors similarly, ranging from 9% to 41%. For these 14 tumors, the linewidths of the LCModel-returned lipid 0.9 and 1.3 ppm peaks were about the same (16.8±4.0 and 16.4±2.2 Hz, respectively), approximately 2.5-fold larger than the tCho linewidth. In addition, the effects of the new fitting method on Glu and GABA estimations were much smaller compared with the 2HG and the differences of Glu and GABA estimates between the two fitting methods were not significantly correlated with the lipid 0.9 ppm signal strength (Figure 4).

ROC (receiver operating characteristic) analysis was performed with the 2HG estimates from the 42 patients, obtained with the two fitting methods. For Fitting method 1, AUC (area under the ROC curve) was 0.977 when the true positive rate (TPR) was plotted versus the false positive rate (FPR) (Figure 5A). A 2HG cutoff corresponding to the point with the smallest distance to the upper-left corner of the ROC curve was obtained as 1.3 mM. Accuracy, sensitivity, and specificity with respect to the biopsy-proven IDH mutational status were calculated as 0.929, 0.913, and 0.947, respectively. The 2HG estimates in 23 IDH mutated tumors were 1.1 – 7.5 mM (3.2±2.0 mM) while the 2HG estimates in 19 IDH wildtype tumors were 0 – 1.8 mM (0.5±0.6 mM) (Figure 5B). For Fitting method-2, AUC was unity (Figure 5C). The 2HG estimates in the 23 IDH mutant tumors ranged from 0.8 to 6.8 mM (2.7±1.8 mM) with CRLB of 3% – 21%, while the 2HG estimates in the 19 IDH wildtype tumors were 0 – 0.4 mM (0.1±0.1 mM) with CRLB ≥ 34% (Figure 5D). Any 2HG cutoff value between 0.4 and 0.8 mM provided a complete distinction between IDH mutation and wildtype (accuracy, sensitivity, and specificity with respect to the IDH status were all 100%).

DISCUSSION and CONCLUSION

The current work reports a spectral fitting strategy for improving *in vivo* ^{1}H MRS evaluation of an oncometabolite 2HG in brain tumors, particularly in tumors with elevated lipids. New lipid basis sets were designed for 3T TE 97 ms MRS and the performance was tested in spectra from 42 glioma patients, in whom the numbers of the biopsy-proven IDH mutated and IDH wildtype tumors were approximately equal. The strength of the lipid 2.25 ppm signal, which appears small in the spectrally crowded region and thus difficult to identify, was preset with reference to the lipid 0.9 ppm signal strength in the basis set. This approach (Fitting method 2) resulted in a complete distinction between IDH mutant and wildtype tumors while the conventional LCModel lipid basis sets did not. This new fitting method, with improvement in 2HG quantification, would provide an effective tool for monitoring 2HG level in longitudinal studies of IDH mutant brain tumors, particularly when the lipid level changes with time.

Our data showed that the 0.9 ppm to 1.3 ppm lipid signal ratio was not the same between patients, suggesting that brain tumors may have several types of fats and the composition of fat types is not identical between tumors. The differential lipid signal ratio between tumors supports our hypothesis that the number of CH_2 chains per fat molecule, which is responsible for the lipid 1.3 ppm signal strength, may differ between tumors while the single CH_3 group, responsible for the 0.9 ppm lipid signal, is present within each fat molecule irrespective of the lipid composition (*i.e.*, independent of the lipid chain length or index of saturation). Thus, the 0.9 ppm signal is preferable as a reference to determine the lipid 2.25 ppm signal strength although the signal is smaller than the lipid 1.3 ppm signal. Compared to fitting with the LCModel built-in lipid basis set (Fitting method 1), a major effect of Fitting method 2 was a decrease in 2HG estimation, which was most likely because the LCModel-returned lipid signal strength at 2.25 ppm was overall larger in Fitting method 2 than in Fitting method 1.

The MM signals were excluded in the spectral fitting of the present study. This may be a reasonable approach since the MM signals in brain tumors have very short T_2 relaxation times[27] and may be negligible at TE 97 ms. When the LCModel built-in MM basis signals were included in the basis set, which was conducted for comparison purpose, 2HG estimates were slightly changed. For the LCModel built-in lipid basis sets, an ROC analysis of the data from fitting with MM basis signals showed a slightly less acceptable result (AUC 0.95, Accuracy 0.905, Sensitivity 0.957, and Specificity 0.842), when compared with the result from without-MM fitting (Fitting method 1). The 2HG estimates in IDH mutated tumors were 1.1 – 8.1 mM (3.3±2.1 mM) while those in IDH wildtype tumors ranged from 0 to 2.1 mM (0.6± 0.6 mM). For our customized lipid basis set, including MM basis signals in the fitting resulted in a complete distinction between IDH mutant and wildtype tumors, similarly as in the without-MM fitting (Fitting method 2). 2HG estimates were overall slightly decreased, leading to a cutoff 2HG of 1.2 mM. The 2HG estimates in IDH mutated tumors were 0.7 – 6.8 mM (2.5±1.8 mM) while those in IDH wildtype tumors ranged from 0 to 0.2 mM (0.03± 0.07 mM). A negative effect of the MM inclusion was that the LCModel-returned baselines showed downward distortions between 0.5 and 2 ppm in some spectra, resulting in apparent overestimation of the lipid 0.9 and 1.3 ppm signals. This prompted us

to conclude that spectral fitting without MM in the basis set may be an appropriate option. In addition, choosing 'tumor' for the LCModel data-type option (sptype), as in the present study, appears to be highly desirable for brain tumor data processing since removing the tumor data type option increased the curvature of the LCModel baseline and did not provide complete differentiation between IDH mutant and wildtype tumors.

The preset lipid signal strengths in our customized lipid basis sets were determined for TE 97 ms according to the data in two prior 7T ^{1}H MRS fat studies in human breast and skeletal adipose tissue.[12, 13] In these studies, the 2.25 ppm to 0.9 ppm lipid signal ratio at TE 20 ms (TR 2 s) was approximately 0.8, which was somewhat larger than their proton number ratio (*i.e.*, 2/3 = 0.67) most likely due to their differential T_1 saturation effects (T_1 = 0.45 and 1.1 s, respectively). The T_2 relaxation time was very different between breast fat and skeletal fatty acids, so we calculated expected 2.25 ppm to 0.9 ppm signal ratios at TE 97 ms separately for breast and skeletal fats using the T_2 values in the two papers and took an average for the present study, which was 1.8/3. The expected lipid signal ratio, calculated with 7T data, should be applicable for 3T. The expected signal strengths of the other customized lipid basis set (LipNew2) were calculated in a similar fashion. In addition, since the preset signal ratios of our customized lipid basis sets were designed for TE 97 ms MRS, the ratios may be applicable for other MRS acquisition methods with similar TE irrespective of field strength. For short-TE MRS data, however, the lipid basis sets of the present study may not be ideal because of the different signal strengths of lipid resonances at short TE. Lipid basis sets can be constructed for short-TE MRS by considering the proton numbers, T_1 difference between resonances, and our proposed strategy to determine the lipid 2.25 ppm signal strength with reference to the lipid 0.9 ppm.

In prior 3T 2HG MRS studies,[14, 15] which used the same MRS sequences as in the present study, false-positive 2HG occurred largely in necrotic tumors, where lipids are elevated. Tietze *et al.* reported, with a cutoff 2HG at 2 mM, two false positive cases in 34 glioma patients.[14] The two false positive 2HG occurred in glioblastomas with elevated lipids. In the study by Suh *et al.*,[15] which was focused on glioblastomas, the false positive rate was as high as 21% (17 cases out of 82), with a cutoff 2HG at 1.8 mM. A multivariable analysis showed that false positive rate was significantly associated with increasing fractional necrosis within the MRS voxels. It is most likely that the incidence of false positive in necrotic tumors may be due to overestimation of 2HG, which can occur when the lipid 2.25 ppm signal is underestimated and the signal at 2.25 ppm is assigned largely to 2HG. When lipid basis signals between 2 and 2.5 ppm are excluded in spectral fitting,[15] the entire lipid signal at 2.25 ppm may be assigned to 2HG. The complication of 2HG evaluation arising from lipid signals may not be alleviated by including the 2HG C2-proton (4.01 ppm) resonance in the spectral fitting because of its signal overlap with the resonances of lactate (4.1 ppm) and myo-inositol (4.06 ppm). Moreover, when the water suppression is poor, the spectral region above 3.5 ppm is often severely distorted and as a result, the 2HG 4.01 ppm signal, which is attributed to a single proton, is very difficult to identify. As a glioma often contains necrotic components within the tumor mass, presence of lipid signals in spectra is practically difficult to avoid when a large cubic voxel is chosen for data acquisition (2×2×2 cm^3)[14, 15] and even when an elongated small voxel is adopted (see Figure 2B). Multivoxel 2HG imaging may have similar issues unless the spatial resolution is very high (*i.e.*, « 1

cm^3). Given these challenges in 2HG evaluation in tumors with high lipids, our proposed strategy to separate 2HG and lipid 2.25 ppm signals in spectral fitting would be useful for minimizing false-positive cases in 2HG MRS.

A major limitation in the present study may be that the lipid basis signals were modeled to be a singlet in spectral analysis, ignoring potential J coupling effects between the fat protons, similarly as in the prior fat MRS studies.[12, 13] This simplification of lipid signal modeling was adopted because accurate values of the lipid J coupling strengths are unknown and the 0.9 ppm signal in spectra from patients exhibited apparently singlet pattern in our *in vivo* spectra, which could be the case of fast decaying signals from J coupled lipid protons. Further improvement in 2HG quantification in high-lipid tumors may be achievable with clarification of lipid J coupling strengths and accurate modeling of lipid basis set for the MRS sequence. Another limitation is the absence of lipid quantification. With the use of long TE, quantification of lipids, whose signals decay fast, requires T_2 relaxation times of brain tumor lipids at 3T, which are unknown. We did not attempt to quantify lipid levels in millimolar units since modeling of the lipid 2.25 ppm signal strength at TE 97 ms was sufficient for 2HG quantification and millimolar quantification of lipids was beyond the scope of the study. In addition, branched-chain amino acids such as valine, leucine, and isoleucine have resonances around 0.9 ppm. In a prior tumor tissue NMR study[28], the concentrations of the amino acids in glioblastomas and grade-III gliomas were about the same as those in grade-II gliomas. Our data showed no measurable signal around 0.9 ppm in grade-II glioma patients. This suggests that the signals at 0.9 ppm in our study, which were detectable in patients with glioblastomas and grade-III gliomas, may be attributed largely to elevated lipids. Lastly, this study was focused on comparison of the new fitting result with the IDH mutational status of the tumors, without direct measurement of the lipid 2.25 ppm signal. Further study is required to evaluate the lipid 2.25 ppm resonance experimentally and examine how the lipid signal interferes with 2HG quantification *in vivo*.

In conclusion, our data suggest that the spectral overlap between the lipid and 2HG signals at 2.25 ppm can be effectively addressed by determining the lipid 2.25 ppm signal with reference to the lipid 0.9 ppm signal intensity. Incorporating our new lipid bases in the spectral fitting may provide a robust fitting strategy for improving MRS identification of IDH mutational status in brain tumors, particularly in necrotic tumors with highly elevated lipids.

Supplementary Material

Refer to Web version on PubMed Central for supplementary material.

ACKNOWLEDGMENTS

We thank Ms. Jeannie Baxter and Kelley Derner for subject recruitment and care of MR scans.

Funding information

National Institutes of Health award R01CA184584

Cancer Prevention Research Institute of Texas (CPRIT) grant RP200456

REFERENCES

1. Dang L, White DW, Gross S, Bennett BD, Bittinger MA, Driggers EM, Fantin VR, Jang HG, Jin S, Keenan MC, Marks KM, Prins RM, Ward PS, Yen KE, Liau LM, Rabinowitz JD, Cantley LC, Thompson CB, Vander Heiden MG and Su SM. Cancer-associated IDH1 mutations produce 2-hydroxyglutarate. Nature. 2009;462:739–44. [PubMed: 19935646]
2. Parsons DW, Jones S, Zhang X, Lin JC, Leary RJ, Angenendt P, Mankoo P, Carter H, Siu IM, Gallia GL, Olivi A, McLendon R, Rasheed BA, Keir S, Nikolskaya T, Nikolsky Y, Busam DA, Tekleab H, Diaz LA Jr., Hartigan J, Smith DR, Strausberg RL, Marie SK, Shinjo SM, Yan H, Riggins GJ, Bigner DD, Karchin R, Papadopoulos N, Parmigiani G, Vogelstein B, Velculescu VE and Kinzler KW. An integrated genomic analysis of human glioblastoma multiforme. Science. 2008;321:1807–12. [PubMed: 18772396]
3. Yan H, Parsons DW, Jin G, McLendon R, Rasheed BA, Yuan W, Kos I, Batinic-Haberle I, Jones S, Riggins GJ, Friedman H, Friedman A, Reardon D, Herndon J, Kinzler KW, Velculescu VE, Vogelstein B and Bigner DD. IDH1 and IDH2 mutations in gliomas. N Engl J Med. 2009;360:765–73. [PubMed: 19228619]
4. Louis DN, Perry A, Reifenberger G, von Deimling A, Figarella-Branger D, Cavenee WK, Ohgaki H, Wiestler OD, Kleihues P and Ellison DW. The 2016 World Health Organization Classification of Tumors of the Central Nervous System: a summary. Acta Neuropathol. 2016;131:803–20. [PubMed: 27157931]
5. Choi C, Ganji SK, Deberardinis RJ, Hatanpaa KJ, Rakheja D, Kovacs Z, Yang XL, Mashimo T, Raisanen JM, Marin-Valencia I, Pascual JM, Madden CJ, Mickey BE, Malloy CR, Bachoo RM and Maher EA. 2-hydroxyglutarate detection by magnetic resonance spectroscopy in IDH-mutated patients with gliomas. Nat Med. 2012;18:624–629. [PubMed: 22281806]
6. Andronesi OC, Kim GS, Gerstner E, Batchelor T, Tzika AA, Fantin VR, Vander Heiden MG and Sorensen AG. Detection of 2-hydroxyglutarate in IDH-mutated glioma patients by in vivo spectral-editing and 2D correlation magnetic resonance spectroscopy. Sci Transl Med. 2012;4:116ra4.
7. Pope WB, Prins RM, Albert Thomas M, Nagarajan R, Yen KE, Bittinger MA, Salamon N, Chou AP, Yong WH, Soto H, Wilson N, Driggers E, Jang HG, Su SM, Schenkein DP, Lai A, Cloughesy TF, Kornblum HI, Wu H, Fantin VR and Liau LM. Non-invasive detection of 2-hydroxyglutarate and other metabolites in IDH1 mutant glioma patients using magnetic resonance spectroscopy. J Neurooncol. 2012;107:197–205. [PubMed: 22015945]
8. Waitkus MS, Diplas BH and Yan H. Biological Role and Therapeutic Potential of IDH Mutations in Cancer. Cancer Cell. 2018;34:186–195. [PubMed: 29805076]
9. Konteatis Z, Artin E, Nicolay B, Straley K, Padyana AK, Jin L, Chen Y, Narayaraswamy R, Tong S, Wang F, Zhou D, Cui D, Cai Z, Luo Z, Fang C, Tang H, Lv X, Nagaraja R, Yang H, Su SM, Sui Z, Dang L, Yen K, Popovici-Muller J, Codega P, Campos C, Mellinghoff IK and Biller SA. Vorasidenib (AG-881): A First-in-Class, Brain-Penetrant Dual Inhibitor of Mutant IDH1 and 2 for Treatment of Glioma. ACS Med Chem Lett. 2020;11:101–107. [PubMed: 32071674]
10. Tugnoli V, Tosi MR, Tinti A, Trinchero A, Bottura G and Fini G. Characterization of lipids from human brain tissues by multinuclear magnetic resonance spectroscopy. Biopolymers. 2001;62:297–306. [PubMed: 11857268]
11. Delikatny EJ, Chawla S, Leung DJ and Poptani H. MR-visible lipids and the tumor microenvironment. NMR Biomed. 2011;24:592–611. [PubMed: 21538631]
12. Dimitrov IE, Douglas D, Ren J, Smith NB, Webb AG, Sherry AD and Malloy CR. In vivo determination of human breast fat composition by (1)H magnetic resonance spectroscopy at 7 T. Magn Reson Med. 2012;67:20–6. [PubMed: 21656551]
13. Ren J, Dimitrov I, Sherry AD and Malloy CR. Composition of adipose tissue and marrow fat in humans by 1H NMR at 7 Tesla. J Lipid Res. 2008;49:2055–62. [PubMed: 18509197]
14. Tietze A, Choi C, Mickey B, Maher EA, Parm Ulhoi B, Sangill R, Lassen-Ramshad Y, Lukacova S, Ostergaard L and von Oettingen G. Noninvasive assessment of isocitrate dehydrogenase mutation status in cerebral gliomas by magnetic resonance spectroscopy in a clinical setting. J Neurosurg. 2018;128:391–398. [PubMed: 28298040]
15. Suh CH, Kim HS, Paik W, Choi C, Ryu KH, Kim D, Woo DC, Park JE, Jung SC, Choi CG and Kim SJ. False-Positive Measurement at 2-Hydroxyglutarate MR Spectroscopy in Isocitrate

Dehydrogenase Wild-Type Glioblastoma: A Multifactorial Analysis. Radiology. 2019;291:752–762. [PubMed: 30990380]

16. Yahya A and Fallone BG. T(2) determination of the J-coupled methyl protons of lipids: In vivo ilustration with tibial bone marrow at 3 T. J Magn Reson Imaging. 2010;31:1514–21. [PubMed: 20512909]
17. Li Y, Srinivasan R, Ratiney H, Lu Y, Chang SM and Nelson SJ. Comparison of T(1) and T(2) metabolite relaxation times in glioma and normal brain at 3T. J Magn Reson Imaging. 2008;28:342–50. [PubMed: 18666155]
18. Madan A, Ganji SK, An Z, Choe KS, Pinho MC, Bachoo RM, Maher EM and Choi C. Proton T2 measurement and quantification of lactate in brain tumors by MRS at 3 Tesla in vivo. Magn Reson Med. 2015;73:2094–9. [PubMed: 25046359]
19. Michaeli S, Garwood M, Zhu XH, DelaBarre L, Andersen P, Adriany G, Merkle H, Ugurbil K and Chen W. Proton T2 relaxation study of water, N-acetylaspartate, and creatine in human brain using Hahn and Carr-Purcell spin echoes at 4T and 7T. Magn Reson Med. 2002;47:629–33. [PubMed: 11948722]
20. Choi C, Ganji S, Hulsey K, Madan A, Kovacs Z, Dimitrov I, Zhang S, Pichumani K, Mendelsohn D, Mickey B, Malloy C, Bachoo R, Deberardinis R and Maher E. A comparative study of short- and long-TE (1)H MRS at 3 T for in vivo detection of 2-hydroxyglutarate in brain tumors. NMR Biomed. 2013;26:1242–50. [PubMed: 23592268]
21. Ogg RJ, Kingsley PB and Taylor JS. WET, a T1- and B1-insensitive water-suppression method for in vivo localized 1H NMR spectroscopy. J Magn Reson B. 1994;104:1–10. [PubMed: 8025810]
22. Provencher SW. Estimation of metabolite concentrations from localized in vivo proton NMR spectra. Magn Reson Med. 1993;30:672–9. [PubMed: 8139448]
23. Thompson RB and Allen PS. Sources of variability in the response of coupled spins to the PRESS sequence and their potential impact on metabolite quantification. Magn Reson Med. 1999;41:1162–9. [PubMed: 10371448]
24. Govind V. 1H-NMR Chemical Shifts and Coupling Constants for Brain Metabolites. eMagRes. 2016;5:1347–1362.
25. Ganji SK, Banerjee A, Patel AM, Zhao YD, Dimitrov IE, Browning JD, Brown ES, Maher EA and Choi C. T2 measurement of J-coupled metabolites in the human brain at 3T. NMR Biomed. 2012;25:523–529. [PubMed: 21845738]
26. An Z, Tiwari V, Baxter J, Levy M, Hatanpaa KJ, Pan E, Maher EA, Patel TR, Mickey BE and Choi C. 3D high-resolution imaging of 2-hydroxyglutarate in glioma patients using DRAG-EPSI at 3T in vivo. Magn Reson Med. 2019;81:795–802. [PubMed: 30277274]
27. Behar KL, Rothman DL, Spencer DD and Petroff OA. Analysis of macromolecule resonances in 1H NMR spectra of human brain. Magn Reson Med. 1994;32:294–302. [PubMed: 7984061]
28. Wright AJ, Fellows GA, Griffiths JR, Wilson M, Bell BA and Howe FA. Ex-vivo HRMAS of adult brain tumours: metabolite quantification and assignment of tumour biomarkers. Mol Cancer. 2010;9:66. [PubMed: 20331867]

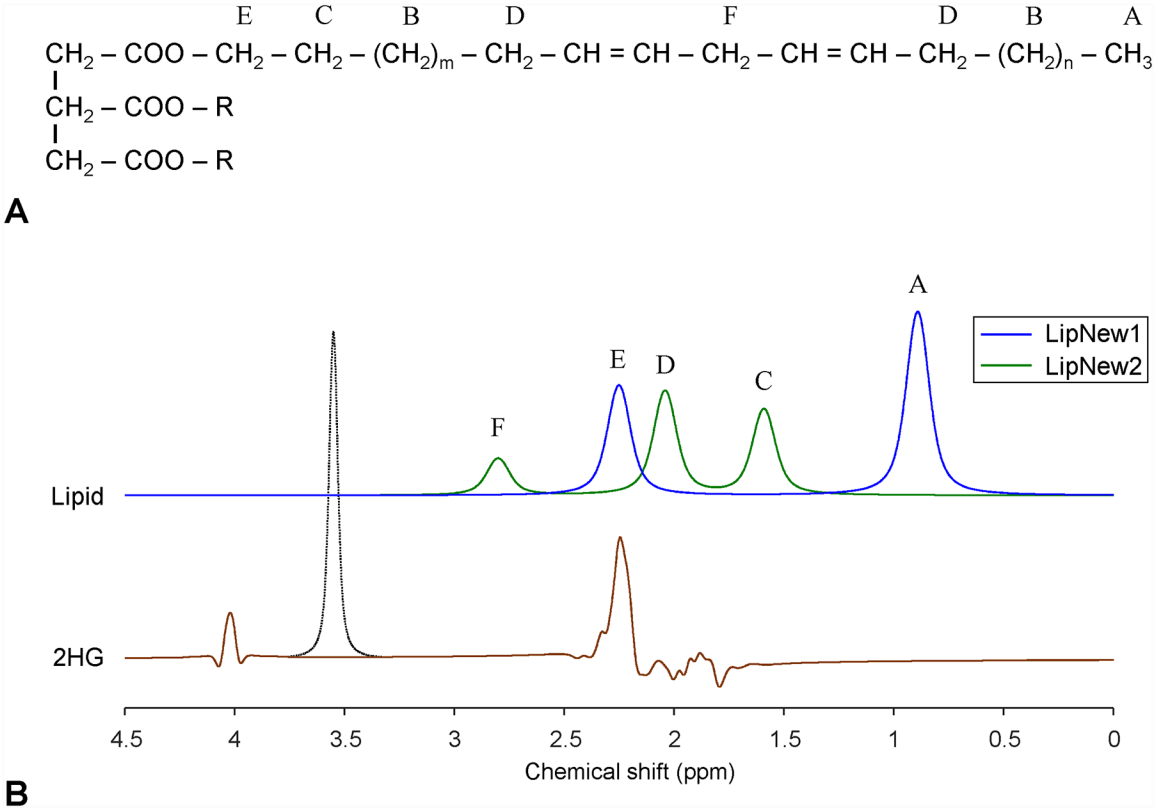

Figure 1.

(**A**) The chemical structure of a triglyceride. The protons resonating between 0.5 and 4 ppm are labeled A to F. (**B**) The signals of new lipid basis sets, LipNew1 and LipNew2, are presented together with a 2HG signal calculated for PRESS TE 97 ms. The lipid peaks were broadened to 16 Hz at half amplitude while the 2HG signal was simulated with 6 Hz singlet FWHM (as indicated in an arbitrary dotted-line singlet). The amplitude ratio of the signals A, E, C, D, and F is 3:1.8:1.4:1.7:0.6.

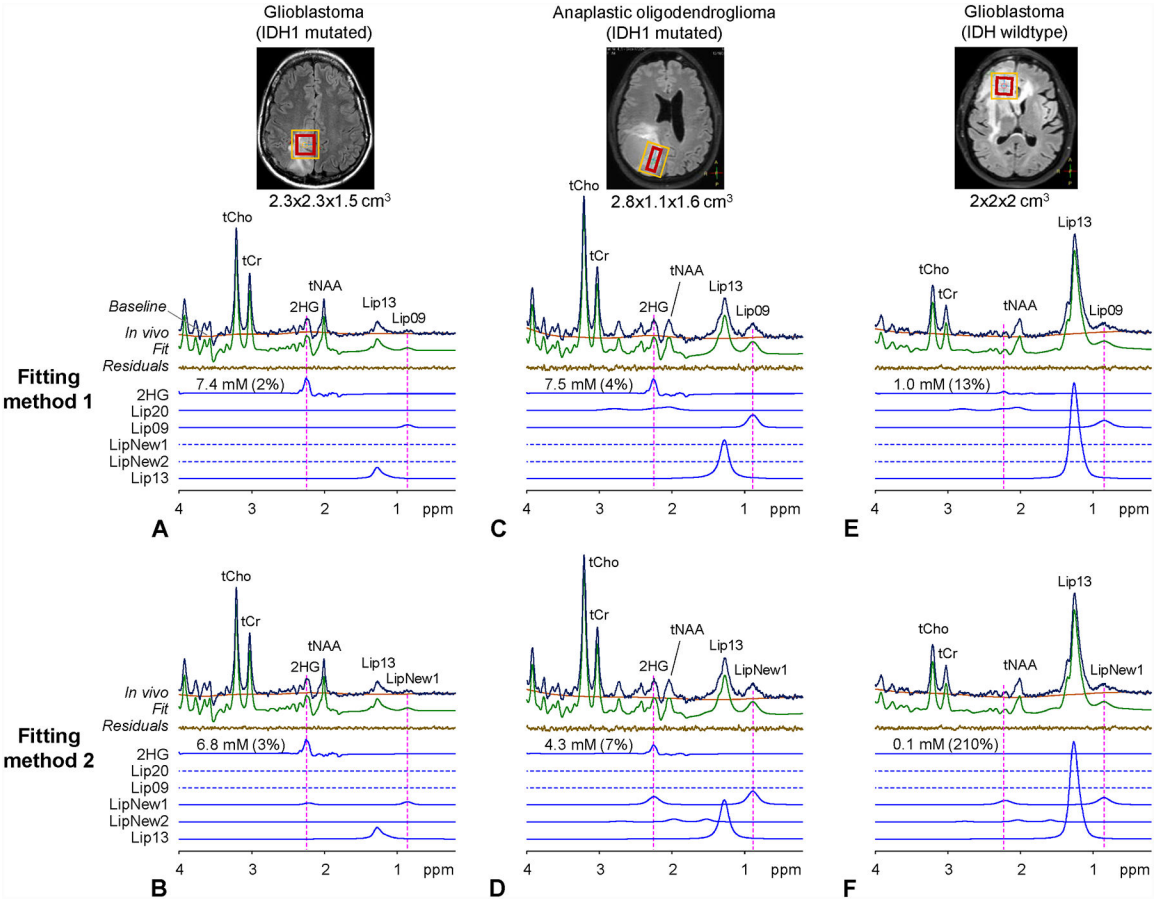

Figure 2.

Representative *in vivo* PRESS TE 97 ms spectra from three glioma patients are presented together with LCModel fitting results and voxel positioning (red line) on T_2-FLAIR images (voxel size shown below the image). The yellow lines denote the shimming volumes, for which the B_1 field was calibrated. LCModel-returned 2HG signals are shown with the estimated millimolar 2HG concentrations and CRLB in brackets. The LCModel built-in lipid basis set (Fitting method 1) included Lip09 (0.89 ppm), Lip20 (2.04, 2.25 and 2.8 ppm), and Lip13 (two signals at 1.3 ppm, *i.e.*, Lip13a + Lip13b). The lipid basis set of Fitting method 2 included LipNew1 (0.9 and 2.25 ppm), LipNew2 (1.59, 2.04, and 2.8 ppm), and Lip13 (Lip13a + Lip13b). Dotted lines denote exclusion of the lipid signals in the basis set. Spectra are scaled with respect to the water signal from the voxel. Vertical lines are drawn at 2.25 and 0.9 ppm.

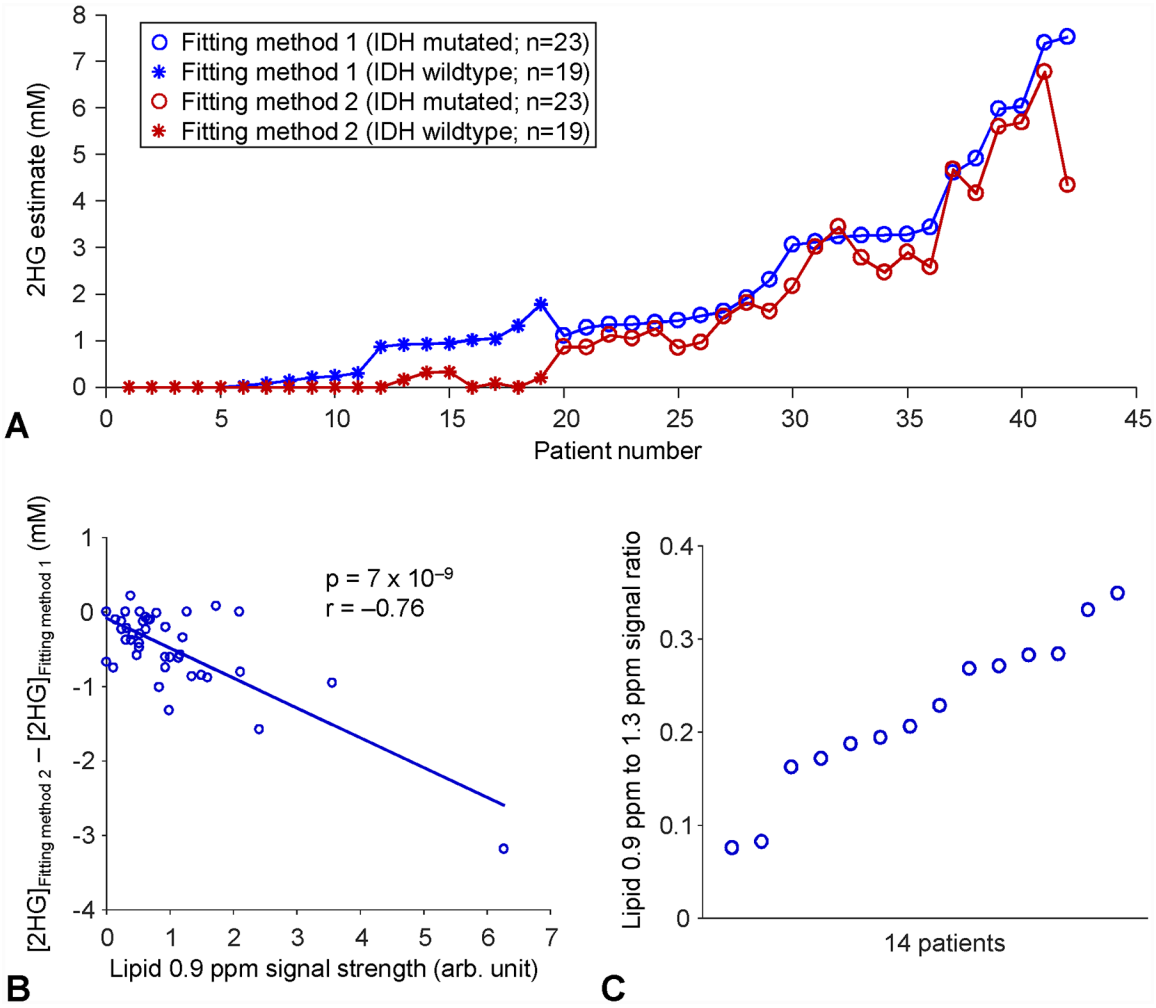

Figure 3.

(**A**) 2HG estimation in 42 patients by Fitting methods 1 (blue) and 2 (red) are displayed in the ascending order of 2HG estimates from Fitting method 1 for each of biopsy-proven IDH mutated (circles) and IDH wildtype (asterisks) tumor groups. Note that the patient number (P1 – P42) in this figure is identical to the patient number in Supporting Information Figure S2. (**B**) Regression analysis of the difference in 2HG estimation between the two fitting methods (*i.e.*, $[2HG]_{\text{Fitting method 2}} - [2HG]_{\text{Fitting method 1}}$) with respect to the lipid 0.9 ppm signal strength. The statistical significance (p) and regression coefficient (r) are shown in the figure. (**C**) The lipid 0.9 ppm to 1.3 ppm peak amplitude ratio, calculated from the LCModel-returned lipid signals, is shown for 14 patients, in whom the lipid 0.9 ppm peak was well discernible (SNR > 4).

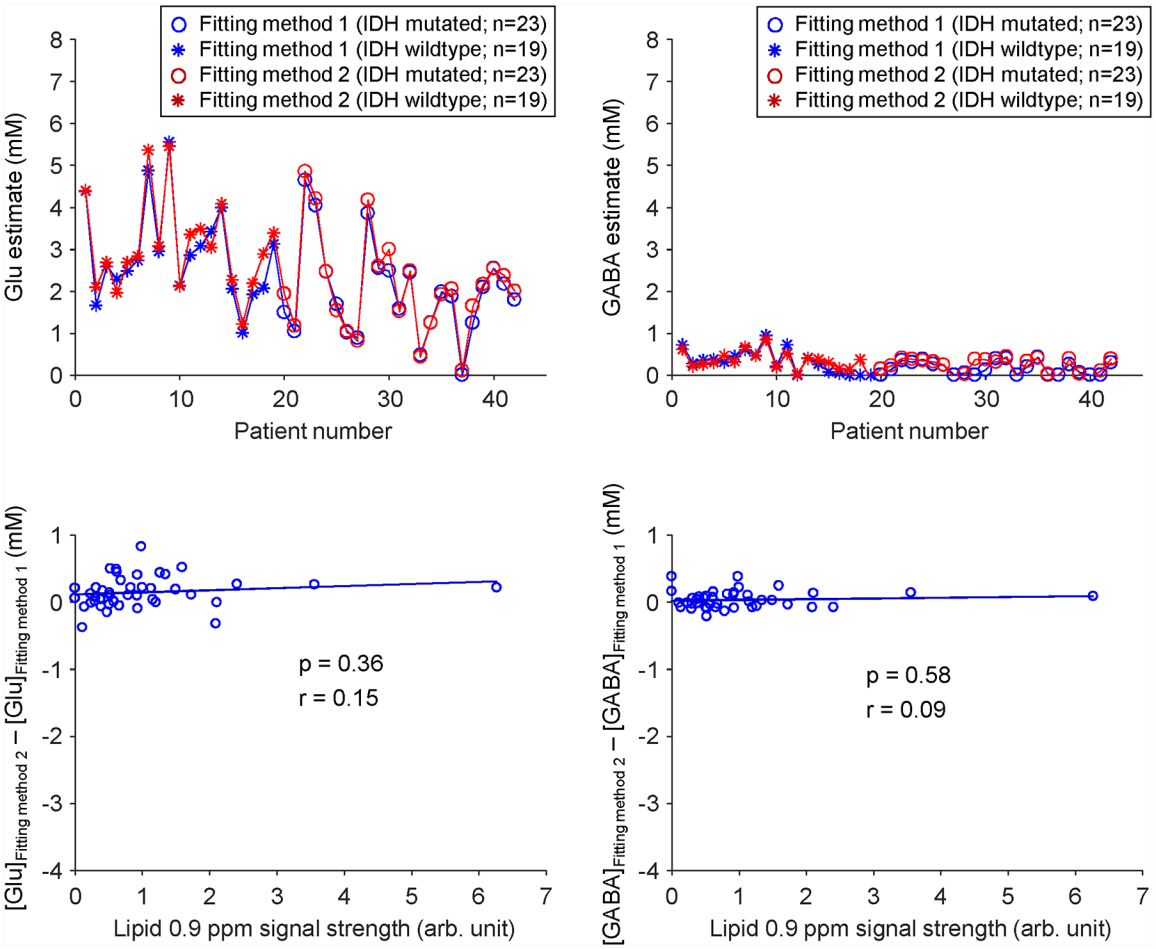

Figure 4.

(**Upper panel**) Glu and GABA estimations in 42 patients by Fitting methods 1 (blue) and 2 (red) are displayed in the same order of subjects as in Figure 3. (**Lower panel**) Regression analyses of the differences of Glu and GABA estimates between the two fitting methods (*i.e.*, $[Glu]_{Fitting\ method\ 2} - [Glu]_{Fitting\ method\ 1}$ and $[GABA]_{Fitting\ method\ 2} - [GABA]_{Fitting\ method\ 1}$) with respect to the lipid 0.9 ppm signal strength. The statistical significance (p) and regression coefficient (r) are shown in the figure.

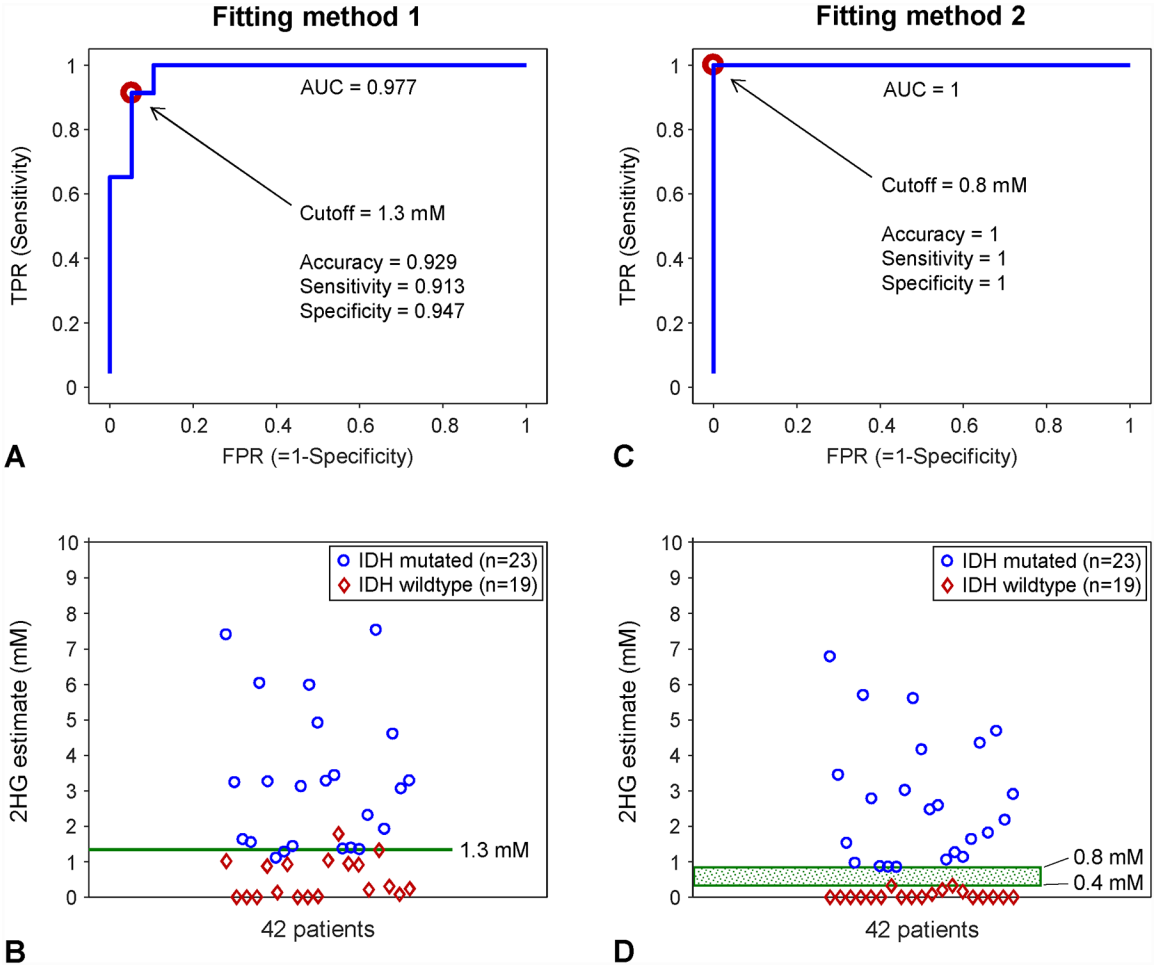

Figure 5.

(**A,C**) Receiver operating characteristic (ROC) analysis of the 2HG estimates from 42 glioma patients is shown for Fitting methods 1 and 2. The area under the curve (AUC) in the plot of true positive rate (TPR) vs. false positive rate (FPR) is shown in the figure. A red circle on a ROC curve corresponds to the smallest distance to the upper-left corner of the curve, at which cutoff values were obtained as 1.3 mM and 0.4 – 0.8 mM for Fitting methods 1 and 2, respectively. Accuracy, sensitivity, and specificity with respect to the IDH mutational status that were calculated with the cutoff values are shown in the figures. (**B,D**) 2HG estimations in the 42 patients by Fitting methods 1 and 2 are displayed according to the IDH mutational status (IDH mutation in blue circles and IDH wildtype in red diamonds). Green lines indicate the threshold values obtained from the ROC curves.